ELSEVIER

Journal of Molecular Catalysis A: Chemical 163 (2000) 9–18

JOURNAL OF MOLECULAR CATALYSIS A: CHEMICAL

www.elsevier.com/locate/molcata

Methane activation on Ni and Ru model catalysts

T.V. Choudhary, D.W. Goodman*

Department of Chemistry, Texas A&M University, College Station, TX 77843-3012, USA

Received 9 February 2000

Abstract

This article reviews research related to the activation of methane by Ni and Ru using model catalysts, highlighting the surface science work carried out using molecular beams methods and elevated pressure reaction studies. Emphasis is placed on connecting the model studies of surface science with the corresponding results obtained on the analogous 'real world' catalysts. These combined studies have added considerable new information to our understanding of the fundamental mechanism of C–H bond activation, the nature of the subsequently formed intermediates and the role these intermediates play in important methane reactions such as steam reforming, partial oxidation and homologation. © 2000 Elsevier Science B.V. All rights reserved.

Keywords: Activation; Catalysts; Partial oxidation; Homologation; Methane activation; Model catalysts; Ni and Ru

1. Introduction

In the last several decades, considerable effort has been directed toward the conversion of methane to value-added products such as transportable liquid hydrocarbons and oxygenates [1–7]. These studies have been motivated by the availability of natural gas (whose main constituent is methane) and the decreasing supply of world petroleum reserves. Methane is a refractory molecule with a C–H bond dissociation energy of 104 kcal/mol and as such, methane activation represents a great challenge to researchers all over the world.

Currently steam reforming of methane represents the primary route for methane conversion [8,9]. This highly endothermic process involves the reaction of methane with steam to form syngas (a mixture of CO and hydrogen). Syngas is reacted to methanol which is then converted to gasoline via the methanol to gasoline (MTG) process [10,11]. The Fischer–Tropsch process can be directly utilized to convert syngas to hydrocarbons [12,13] whereas direct conversion of methane to hydrocarbons can be carried out via the oxidative coupling of methane [14]. Though many researchers have contributed toward significant improvements in methane coupling [15–18], it is still far from being a commercially viable process. In recent years, a two step non-oxidative low temperature methane homologation process (comprising of methane chemisorption in the first step followed by hydrogenation of a hydrocarbonaceous species to hydrocarbons in the second step) has been proposed [19,20]. unfortunately the hydrocarbon yields obtained thus far are too low for the process to be economically viable. Very recently we have proposed, in similar fashion, the step-wise steam reforming of methane over Ni based catalysts for production of CO-free hydrogen for use in fuel cells [21,22].

* Corresponding author. Tel.: +1-409-845-0214;
fax: +1-409-845-6822.
E-mail address: goodman@mail.chem.tamu.edu (D.W. Goodman).

PII: S1381-1169(00)00395-2

Ultimately in order to optimize the development of superior catalysts, it is essential to understand the catalyst surface at the molecular level. Over the past two decades there have been an emergence of a number of spectroscopic tools which enable comprehensive characterization of a catalyst surface at the atomic level [23–25]. These techniques have provided new insights into phenomena such as chemisorption on metal surfaces, adsorbate–adsorbate interactions and reactions.

In this review studies related to methane activation on Ni and Ru single crystals are summarized. The interaction of methane with Ni surfaces is of considerable importance because steam reforming of methane is carried out on Ni-based catalysts [8]. The interest in Ru arises from the fact that Ru-based catalysts are very active for the two step methane homologation process [19].

2. Methodologies and techniques employed

In this section a brief description is given of the various methodologies and surface science techniques that have been utilized for the investigations to be described. Both 'molecular beam techniques' and 'bulb methods' have been extensively used to acquire a wide range of information relevant to methane dissociation on surfaces. Molecular beam techniques are relatively new and permit considerable control with respect to reactant parameters such as translational kinetic energy and incident angle. The beam energy can be varied by changing the nozzle temperature or by seeding of the methane beam with H_2 or inert gases such as He and Ar. The molecular beam approach was first employed to study methane dissociation by Rettner and co-workers, who utilized translational kinetic energy to overcome the activation barrier for methane dissociation on W(1 1 0) surfaces [26]. Since this pioneering work, molecular beam methods have been regularly used as a probe for investigating methane dissociation on various surfaces [27–31].

However, it is rather difficult to generate a molecular beam with very low kinetic energies and with sufficient flux to measure dissociative sticking at very low sticking probabilities ($<10^{-7}$, such as those typically encountered in 'real world' methane dissociation, e.g. steam reforming of methane). In typical elevated pressure catalytic processes, the major fraction of the molecules has a rather low translational energy, e.g. a mean temperature of 850–1000 K.

A notable drawback of surface science techniques is their applicability only under ultra-high vacuum (UHV) conditions, conditions far removed from the real world catalytic processes typically operated at atmospheric pressures or greater [32]. This limitation has been overcome by combining in a single apparatus an elevated pressure reactor and an UHV surface analysis chamber [33–35]. In most of the 'bulb experiments' the sample under investigation is exposed to high incident fluxes of methane (up to several Torr) in a elevated-pressure reactor and surface analysis then subsequently performed in a contiguous UHV chamber. This approach has facilitated a direct comparison of reaction rates measured on single crystal surfaces with those measured on 'real world catalysts' and has allowed detailed studies addressing reaction mechanisms, structure/activity relationships and the effect of promoters/inhibitors on catalytic activity [32].

The following surface science techniques have been used for surface analysis in the following studies to be discussed:

1. Auger electron spectroscopy (AES) and X-ray photoelectron spectroscopy (XPS) for surface composition and quantitative information on surface species;
2. low energy electron diffraction (LEED) for determination of the structure of the single crystal and ordered adsorbate layers;
3. scanning tunneling microscopy (STM) for imaging the local surface topography with atomic resolution;
4. high resolution electron energy loss spectroscopy (HREELS) to identify the adsorbed species.

3. Studies undertaken on Ni single crystals

The dissociation of methane is considered to be the rate-limiting step in the steam reforming of methane. This has led to a great interest in investigating the fundamental sticking process of methane on Ni single crystals. Almost two decades ago, Bootsma and co-workers showed that methane did not adsorb on Ni(1 1 0) at room temperature without the aid of an electron excitation sources [36]. The interaction

of methane with the low index Ni surfaces was investigated at low pressures (10^{-4}–10^{-2} Torr) using AES and LEED [36–38]. The sticking coefficient for methane on Ni(1 1 0) was observed to be on the order of 10^{-8} at temperatures between 473–579 K. The authors proposed two possible kinetic decomposition processes for methane dissociation on Ni(1 1 0) with activation energies of 21 and 31 kcal/mol but refrained from distinguishing between the two due to the limited experimental accuracy of their kinetic results [36]. A nucleation and growth model for carbon deposition was proposed involving the capture of the mobile carbon species at the periphery of nickel carbide islands. No detectable methane adsorption activity was found on the Ni(1 1 1) surface ($<1 \times 10^{-10}$) whereas a sticking coefficient of $\sim 5 \times 10^{-9}$ was measured for the CH_4/Ni(1 0 0) system [38]. Also for CH_4/Ni(1 0 0), the initial rate of methane decomposition was found to be comparable at 474 and 503 K suggesting a non-activated mechanism. Methane dissociation on Ni(1 0 0) produced two different surface carbides, the β and γ forms (γ was found to be more stable and the more tightly bound of the two forms).

In contrast to Bootsma and co-workers, who used low methane pressures (10^{-4}–10^{-2} Torr), Beebe et al. investigated the kinetics of methane decomposition on Ni(1 1 1), Ni(1 1 0) and Ni(1 0 0) using a relatively high incident methane flux (1 Torr) [39]. This increase in pressure from the studies of Bootsma and coworker provided sufficient pressure to yield an equilibrated gas layer (with a thickness of several gas mean free paths) around the heated single crystal. Kinetic experiments were performed in a high-pressure reaction cell with surface characterization via AES in a contiguous UHV chamber subsequent to reaction. Fig. 1 shows the carbon build up on the low index planes of Ni as a function of time at 450 K. The reaction probability of methane was the highest on Ni(1 1 0) and the lowest on Ni(1 1 1). The curved nature of the plots for Ni(1 1 1) and Ni(1 0 0) are consistent with a strong coverage dependence of the surface carbon for the methane reactive sticking. The linear behavior of the data for Ni(110), however suggested the formation of islands of surface carbon and/or a much lower dependence of the reaction on surface carbon coverage. The apparent activation energies for methane decomposition were found to be 12.6, 13.3 and 6.4 kcal/mol for Ni(1 1 1), Ni(1 1 0) and Ni(1 0 0), respectively. Kinetic studies

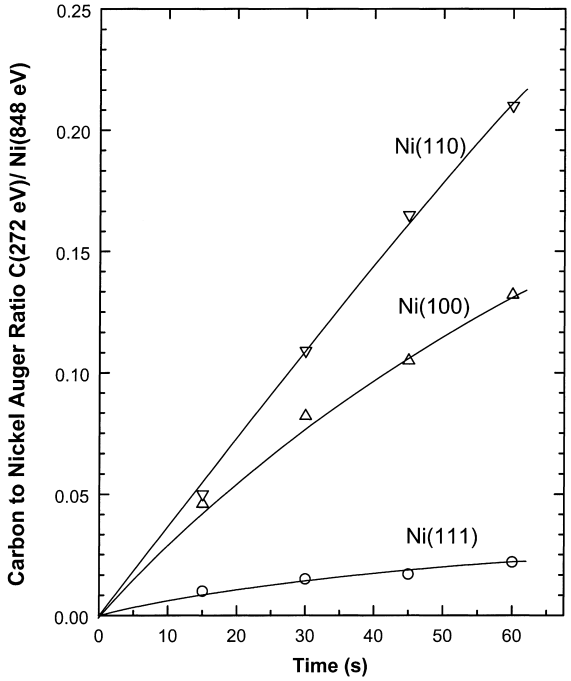

Fig. 1. Methane decomposition kinetics on low index planes of Ni single crystal surfaces at 450 K and 1 Torr methane pressure [39].

employing deuterated methane showed a large kinetic isotopic effect for Ni(1 0 0) whereas no such effect was observed for the Ni(1 1 0) surface. The importance of the surface structure for the methane decomposition reaction was apparent in the observed differences found for the initial sticking probabilities for methane on the different surfaces (summarized in Table 1).

The reaction rates measured by Beebe et al. were found to be an order of magnitude higher than the steady state rates measured for steam reforming of methane (taking into account the difference in experimental conditions) [8]. This difference was rationalized by the fact that the methane reactive sticking rates measured in this investigation were initial rates (i.e. on

Table 1
Initial thermal sticking coefficients for methane at 500 K [39]

System	Sticking coefficient
CH_4/Ni(1 1 1)	1×10^{-8}
CH_4/Ni(1 0 0)	6×10^{-8}
CH_4/Ni(1 1 0)	1×10^{-7}

a clean surface) as opposed to steady state rates. On the other hand, the contradictory results observed by Bootsma and co-workers [36–38] (lower sticking coefficients, non-activated behavior for Ni(1 0 0)) were explained as due to a nonequilibrated gas above the Ni single crystal surfaces at the lower methane pressures employed in these studies.

Ceyer and co-workers investigated the CH_4/Ni(1 1 1) system using molecular beam techniques and HREELS [27]. Both translational and vibrational energy were found to exponentially increase the probability for methane dissociation on Ni(1 1 1). The authors proposed a translationally/vibrationally activated tunneling mechanism for the dissociation of methane on Ni(1 1 1) surface similar to that suggested by Rettner and coworkers for methane reactive sticking on tungsten. The absolute value of the sticking coefficients and the activation energy observed for CH_4/Ni(1 1 1) system found in this study were in good agreement with the bulb experiments carried out by Beebe et al. [39]. In a second molecular beam study, Hamza and Madix reported a linear dependence of methane reactive sticking as a function of translational energy with a considerably larger sticking coefficients (two to three order magnitude) at a given incident energy for the CH_4/Ni(1 0 0) system [40], this was in marked contrast to the exponential dependence measured by Ceyer and co-workers for the CH_4/Ni(1 1 1) system [27].

In subsequent experiments Ceyer and co-workers showed that collision of inert gas molecules with physisorbed CH_4 on Ni(1 1 1) at 46 K resulted in the dissociation of methane [41]. The methyl groups resulting from the dissociation of methane were detected by HREELS. The authors proposed a 'hammer' model to explain the above phenomena, i.e. an impulsive transfer of kinetic energy from Ar or Ne to adsorbed methane. This impulsive energy transfer was consistent with the mass dependence of the inert gas used, a result inconsistent with a non-impulsive energy transfer model. In an extension of this work the Ceyer group carried out the synthesis of benzene on Ni(1 1 1) [42,43] by first physisorbing methane at 47 K, then bombarding the methane with Kr atoms. This led to the formation of adsorbed CH_3 and H species which upon raising the surface temperature, yielded benzene via a C_2H_2 intermediate as determined by HREELS.

Yates and co-workers investigated the effect of an inert gas diluent on the reactive sticking of methane on a Ni(1 1 1) single crystal surface [44]. Total carbon deposition formed via methane decomposition (at constant total methane fluence) was found to increase with increasing methane pressure. Below a threshold pressure of 0.2 Torr no dissociation of methane was observed. The results were consistent with methane dissociation proceeding on Ni(1 1 1) via a direct dissociative mechanism (dissociation on impact) rather than a precursor mediated mechanism (which involves a precursor/trapped state accommodated to the surface at the surface temperature) [45]. The carbon deposition efficiency was calculated to be 4×10^{-8} C atoms per collision (of CH_4) at 1 Torr pressure and 600 K. Mixtures of 10% methane with neon/argon showed significant carbon decomposition at 0.75 Torr total pressure (partial pressure of methane: 0.075 Torr) whereas no carbon deposition was observed with pure methane at a pressure of 0.075 Torr. The authors proposed that the excitation of methane occurred either by collision with the Ni(1 1 1) surface or with hot gas molecules and that the methane molecule then underwent dissociation upon re-impacting the surface.

Sulfur is a well-known poison of Ni catalysts and thus understanding the role of this surface modifier is of considerable importance in the quest for more sulfur-tolerant Ni catalysts. With this objective our laboratory undertook the investigation of the effect of sulfur on the dissociation of methane on a Ni(1 0 0) surface [46]. Ni(1 0 0) was chosen in order to compare such data with our previous work addressing the effect of sulfur on CO methanation on Ni(1 0 0) [47,48]. Fig. 2 shows the initial methane decomposition rate (at 1 Torr methane) as a function of sulfur coverage, calibration of the sulfur coverage was accomplished by using the S/Ni Auger ratio [49]. Comparison with data on clean Ni(1 0 0) surface [39] revealed that a very small coverage of sulfur (<0.01 ml) did not exert a significant influence on the decomposition rate. However, at higher coverages, sulfur had a significant detrimental effect on the initial decomposition rate in that the rate dropped essentially to zero at a sulfur coverage of $\sim$0.3 ml. The linear data as seen in the figure was fit to a simple first order Langmurian form.

$S(\theta_s) = S_0(1 - \alpha\theta_s)$ where θ_s is the sticking probability of methane at a given sulfur coverage θ_s, S_0 is the methane sticking probability on the clean surface

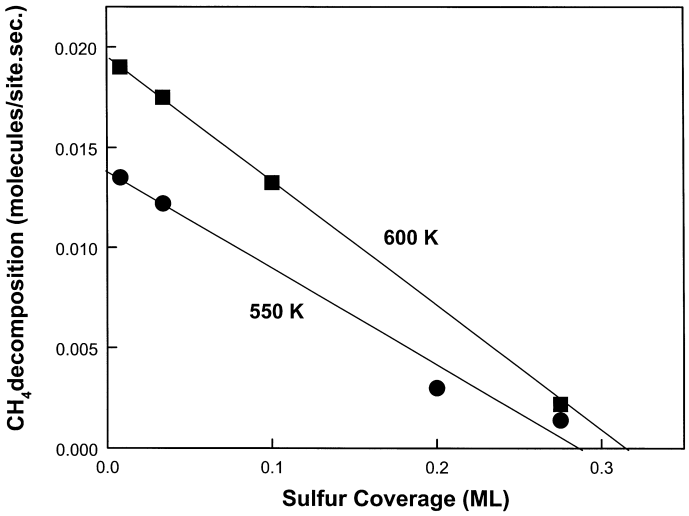

Fig. 2. Effect of sulfur coverage (ml) on the initial methane decomposition rate [46].

and α denotes the number of dissociation sites blocked by each sulfur atom. The experimental data indicated that each sulfur atom was responsible for blocking three sites for methane activation. This was found to be in excellent agreement with the molecular beam experiments of Hamza and Madix whose work indicated the requirement of three sites for methane decomposition on Ni(1 0 0) [40]. In previous work, Frennet and co-workers had speculated that methane decomposition required as many as approximately seven sites on rhodium [50]. Previous studies in our laboratories had shown that sulfur exhibited 'long range' electronic effects for the CO methanation reaction in that 10 or more nickel sites were deactivated by a single sulfur atom [47].

Bulb experiments in our lab indicated that methane dissociation on Ni(1 0 0) proceeded predominantly via a precursor mediated mechanism with only a small contribution from a direct dissociation mechanism [51]. This was in conflict with work by Chorkendorff and co-workers who observed that direct dissociation mechanism was dominant [52,53]. Our group also investigated methane decomposition on NiO thin films. The preparation of these films involved dosing of a Ni(1 0 0) substrate with 300 l of O_2 at ~325 K and further annealing to 600 K for 1 min. The reaction probabilities for methane dissociation on Ni(1 0 0), NiO/Ni(1 0 0) and NiO powder [54] are plotted in Fig. 3 as a function of reciprocal temperature. The methane reactivity on NiO films was found to be larger than on NiO powder but smaller than that on a clean Ni(1 0 0) surface. The apparent activation

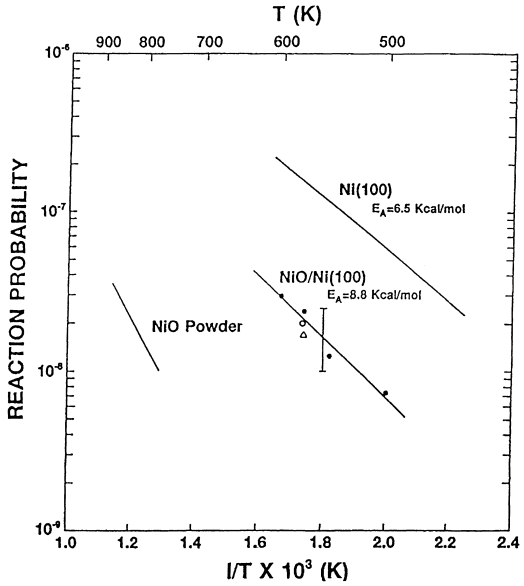

Fig. 3. Temperature dependence of the methane reaction probability for NiO/Ni(1 0 0) thin films [51], Ni(1 0 0) [39] and NiO powder [54]. The data for methane oxidation on NiO powder is for 25% methane, 12.5% O_2, 67.5% Ar, 1 atm total pressure.

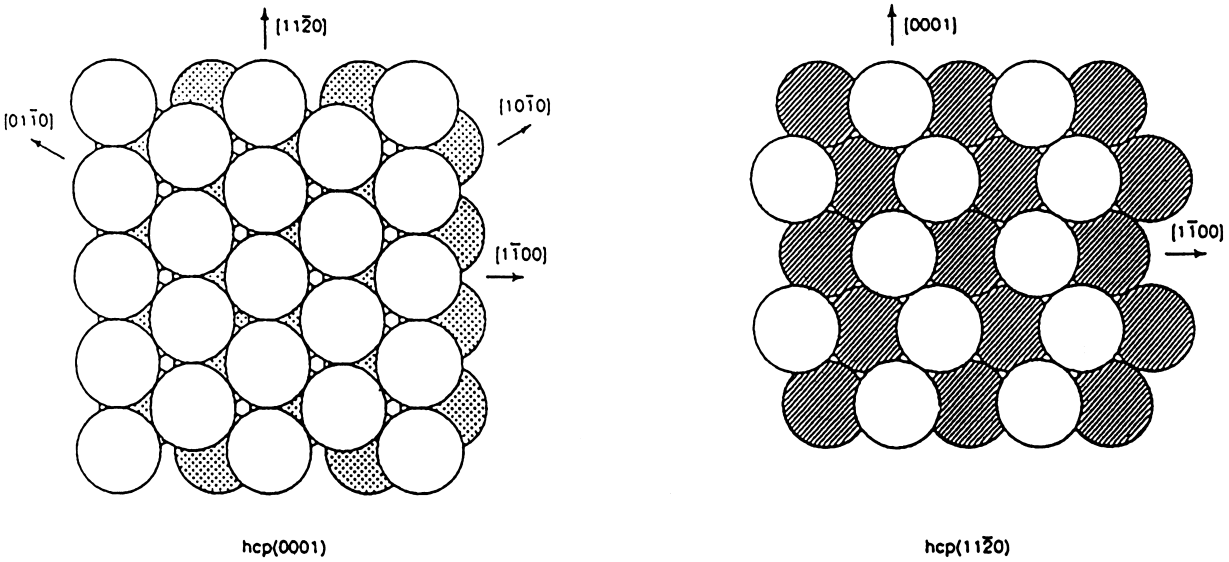

Fig. 4. Surface structures for Ru(0 0 0 1) and Ru(1 1 $\bar{2}$ 0) [58].

energy for the CH_4/[NiO/Ni(1 0 0)] system was found to be 8.8 ± 1.1 kcal/mol and was comparable to that for the CH_4/Ni(1 0 0) system. Based on this similarity the authors proposed that the activation of methane occurred at metallic Ni sites on the NiO film. Scanning tunneling microscopy studies do in fact, reveal a Ni defect density of 20–25% for NiO [55] consistent with the order of magnitude lower methane reaction probability for the NiO/Ni(1 0 0) relative to Ni(1 0 0).

Very recently Juurlink et al. used an elegant experimental approach to unravel the mechanism for methane decomposition on Ni(1 0 0) [56]. They utilized infrared laser excitation of molecules in supersonic molecular beam to achieve vibrational excitation of methane by the ν_3 antisymmetric C–H stretching vibrational mode. For all translational energies employed, singular excitation of ν_3 resulted in a large enhancement in dissociative chemisorption of methane. Comparison studies showed that the translational energy was more effective in enhancing the sticking probability than the vibrational excitation of ν_3.

4. Investigations undertaken on Ru model catalysts

In recent years, the non-oxidative low temperature homologation of methane has been proposed as an alternative to oxidative coupling of methane [19,20]. The process involves methane decomposition in a first step followed by hydrogenation of the surface carbonaceous species in a second step to obtain C_{2+} hydrocarbons. Ru was found to be a particularly suitable catalyst for this process [57]. To better characterize this process our laboratories studied this reaction sequence on Ru catalysts consisting of model single crystal surfaces as well as the high surface area supported counterpart. Fig. 4 shows schematically the Ru(0 0 0 1) and Ru(1 1 $\bar{2}$ 0) surfaces [58]. The single crystals were cleaned in the UHV spectroscopic chamber and subsequently transferred to a high-pressure reaction chamber via a double-stage differentially pumped teflon sliding seal. Methane dissociation on the Ru single crystal was carried out in the reaction chamber subsequent to which the surface species were detected by HREELS in the UHV chamber. Fig. 5 shows the HREELS spectra subsequent to methane decomposition on Ru(1 1 $\bar{2}$ 0) as a function of reaction temperature. The large body of HREELS data related to hydrocarbon decomposition on various transition metals was utilized to relate the HREELS signal to various surface species [1]. The features at 830 and 3010 cm^{-1} (observed in the temperature range

[1] All related literature cited in [58].

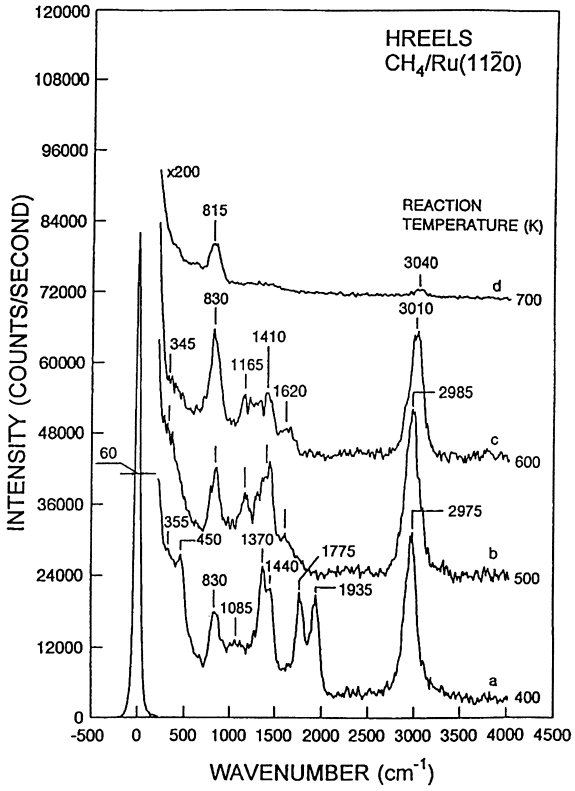

Fig. 5. HREELS spectra obtained following methane decomposition on Ru(1 1 $\bar{2}$ 0) (5 Torr methane for 120 s) as a function of reaction temperature [58]. The spectra was collected at $E_p \sim 2.2$ eV and at the spectrally reflected beam direction.

of 400–700 K) were attributed to a methylidyne (CH) species. The loss features at 345, 1165, 1410, 1620 and 2985 cm^{-1} were assigned to a vinylidene (CCH_2) species. The third set of loss features consisting of the features at 355, 1085, 1370, 1440 and 2975 cm^{-1} correspond to the ethylidyne (CCH_3) species. In contrast methane decomposition on Ru(0 0 0 1) yielded only the methylidyne and vinylidene species. For both substrates, only the graphitic phase of carbon was observed above 700 K.

The kinetics of the two step methane homologation reaction was investigated in a separate chamber equipped with a gas chromatograph along with AES and TPD [59,60]. The reaction sequence used for the two step process was as follows:

1. dissociation of methane was carried out in the high-pressure reaction-cell at the desired temperature for 5 min;
2. the methane was pumped away and the temperature of the crystal was lowered simultaneously;
3. after hydrogenation for 10 min the product gas-mixture was detected with a flame ionization detector.

Under these experimental conditions the maximum yield in ethane/propane was obtained at 500 K (first step temperature) on both Ru(0 0 0 1) and Ru(1 1 $\bar{2}$ 0) single crystal catalysts. Optimum reaction conditions resulted in the production of 16% ethane and 2% propane. The ethane/propane yield maximized at a hydrogenation temperature (second step) of 400 K on Ru(0 0 0 1) whereas no such maximum was observed on Ru(1 1 $\bar{2}$ 0). HREELS studies in parallel had shown that four species, i.e. methylidyne (CH), vinylidene (CCH_2), ethylidyne (CCH_3) and graphitic species were observed on Ru(1 1 $\bar{2}$ 0) after the methane decomposition step. However, only three species (CH, CCH_2 and graphitic) were observed for the Ru(0 0 0 1) surface [58].

The vinylidene species were proposed to be the dominant precursors for C_2 production since:

1. the maximum in HREELS intensities of the vinylidene species (rather than the methylidyne species) coincided with the maximum in ethane/propane production;
2. the hydrogenation of the vinylidene species to ethane was expected to be more facile than the polymerization and hydrogenation of the methylidyne species to ethane.

Based on the HREELS and kinetic studies the following reaction mechanism was proposed for methane coupling on Ru surfaces (shown in Fig. 6) [60]. Dissociative methane chemisorption in the first step between 400–600 K results in the formation of methylidyne and vinylidene species on the Ru surface. The methyl-

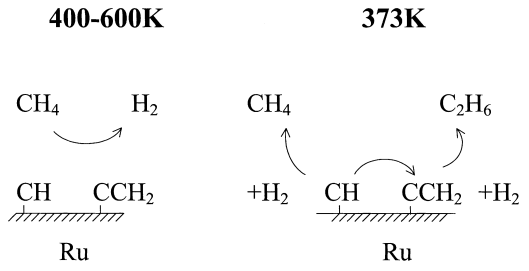

Fig. 6. Schematic diagram for the reaction mechanism for methane coupling on Ru surfaces [60].

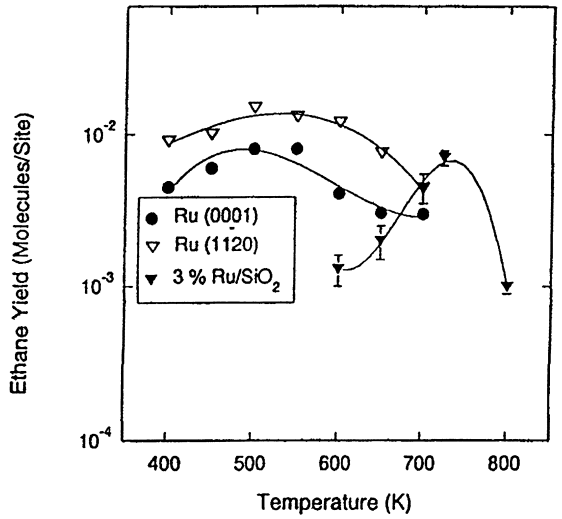

Fig. 7. Comparison of ethane yields for single crystal surfaces [59] and supported Ru catalysts (conditions used were: GHSV (methane) = 6000 h^{-1}, total methane input = 4.8 μmol, T (H_2) = 368 K, GHSV (H_2) = 2000 h^{-1}.

idyne intermediates are then directly hydrogenated to methane or polymerized to vinylidene species. Hydrogenation of these vinylidene species finally results in the production of ethane.

These studies included the study of the coupling reaction on a silica supported Ru catalyst [61]. It is noteworthy that the ethane yields for the high area supported catalyst and the single crystals were comparable (same order of magnitude). The comparison of the ethane yields as a function of temperature for both systems are shown in Fig. 7. For the supported Ru catalyst the maximum of the ethane yield shifted toward higher temperatures relative to the single crystals. The yield for ethane optimized at 30–35% carbon coverage and was about 13–15%.

Earlier HREELS studies in our laboratories showed the presence of only the graphitic phase on both Ru(1 1 $\bar{2}$ 0) and Ru(0 0 0 1) surfaces after methane dissociation above 700 K [58]. The nature of these inactive carbonaceous species was studied using HREELS, STM and LEED [62]. In these studies the methane decomposition was carried out in the high-pressure cell at 800 K at a methane pressure of 10 Torr. STM measurements were then carried out ex situ after completion of the reaction. The STM images indicate the presence of small carbonaceous clusters on the surface with a diameter and apparent height of ∼10–15 and ∼2–3 Å, respectively These clusters were adsorbed on lower terraces of the step edges of the surface and were evenly distributed inside carbon islands. The HREEL spectrum was also found to be consistent with the presence of small carbon clusters. LEED studies suggested that the individual carbon atoms (within the clusters) were preferentially oriented along the ⟨0 0 0 1⟩ plane of Ru. On Ru(1 1 $\bar{2}$ 0), the carbon atoms formed from methane decomposition at 800 K nucleated to form three-dimensional particles of graphite. This difference in growth patterns of carbon atoms was attributed to the structural differences between the two substrates.

The substrate signal is known to interfere with the detection of fractional monolayers of carbon (by AES [63] and XPS [64]) on the Ru surface. To circumvent this, the δ (CH) intensity obtained from HREELS was utilized to estimate the sticking probability of methane on Ru(0 0 0 1) [65]. The measured sticking co-efficients varied from 10^{-6} to 10^{-7} in the temperature range 500–650 K. Fig. 8 shows the comparison of methane sticking coefficients on Ru(0 0 0 1) and low index planes of Ni crystals. The apparent activation energy for the methane decomposition on Ru(0 0 0 1) was estimated to be 8.5 kcal/mol. This value was in reasonable agreement with the methane dissociation activation energy (6.2 kcal/mol) on Ru-silica catalysts

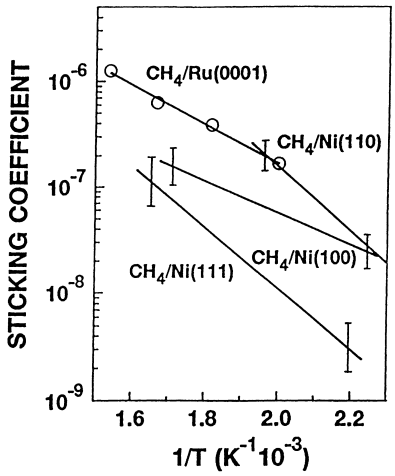

Fig. 8. Methane sticking coefficients for CH_4/Ru(0 0 0 1) [65]. Included for comparison are those measured from low index planes of Ni crystals [39].

[66]. Molecular beam studies carried out by Larsen et al. on the same system also showed excellent agreement for the activation energy measurements (∼8.8 kcal/mol) [31].

5. Concluding remarks

These investigations using a variety of model catalysts have clearly illustrated the efficacy of model catalyst studies in providing a greater understanding of the methane activation process. Ni single crystal studies have shown methane dissociation to be structure sensitive and thus have contributed to the solution of a fundamental question in heterogeneous catalysis. Important information regarding sulfur as a surface modifier has been obtained via these model studies. Investigation of methane homologation on Ru model catalysts has been successful in determining the intermediate surface species and in implicating a particular reaction mechanism.

It is apparent that catalysis and surface science are complementary disciplines and an integrated approach will continue to contribute to the understanding of the vastly complex world of heterogeneous catalysis.

Acknowledgements

We acknowledge with pleasure the support of this work by the Department of Energy, Office of Basic Sciences, Division of Chemical Sciences and the Robert A. Welch Foundation.

References

[1] J.R. Anderson, Appl. Catal. 47 (1989) 177.
[2] J.H. Lunsford, Catal. Today 6 (1990) 235.
[3] V.R. Choudhary, S.T. Chaudhari, V.H. Rane, A.M. Rajput, J. Chem. Soc., Chem. Commun. (1989) 555.
[4] N.D. Parkyns, C.I. Warburton, J.D. Wilson, Catal. Today 18 (1993) 385.
[5] P. Qiu, J.H. Lunsford, M.P. Rosynek, Catal. Lett. 48 (1997) 11.
[6] Y.D. Xu, L.W. Lin, Appl. Catal. A: Gen. 188 (1999) 53.
[7] V.R. Choudhary, A.M. Rajput, B. Prabhakar, Angew. Chem. Int. Ed. Engl. 33 (1994) 2104.
[8] J.R. Rostrup-Nielsen, Catalytic steam reforming, in: J.R. Anderson, M. Boudart (Eds.), Catal. Sci. Eng., Vol 5, Springer, Berlin, 1984.
[9] J.R. Rostrup-Nielsen, Catal. Today 18 (1993) 305.
[10] C.D. Chang, Catal. Rev. Sci. Eng. 25 (1983) 1.
[11] F.J. Keil, Micropor. Mesopor. Mat. 29 (1999) 49.
[12] M.A. Vannice, Catal. Rev. Sci. Eng. 14 (1976) 153.
[13] G.P. Van der Laan, A.A.C.M. Beenacker, Catal. Rev. Sci. Eng. 41 (1999) 255.
[14] G.E. Keller, M.M. Bhasin, J. Catal. 73 (1982) 9.
[15] J.H. Lunsford, Angew Chem. Int. Ed. Engl. 34 (1995) 970.
[16] V.R. Choudhary, S.T. Chaudhari, M.Y. Pandit, J. Chem. Soc., Chem. Commun. (1991) 1158.
[17] A.L. Tonkovich, R.W. Carr, R. Aris, Science 262 (1993) 221.
[18] Y. Jiang, I.V. Yentekakis, C.G. Vayenas, Science 264 (1994) 1563.
[19] T. Koerts, R.A. Van Santen, J. Chem. Soc., Chem. Commun. (1991) 1281.
[20] M. Belgued, P. Pareja, A. Amariglio, H. Amariglio, Nature 352 (1991) 789.
[21] T.V. Choudhary, D.W. Goodman, Catal. Lett. 59 (1999) 93.
[22] T.V. Choudhary, D.W. Goodman, J. Catal. 192 (2000) 316.
[23] G.A. Samorjai, Chemistry in Two Dimensions: Surfaces, Cornell University Press, Ithaca, NY, 1981.
[24] G. Ertl, J. Kuppers, Low Energy Electrons and Surface Chemistry, VCH Verlagsgesellschaft, Weiheim, 1985.
[25] D.P. Woodruff, T.A. Delchar, Modern Techniques of Surface Science, Cambridge University Press, NY, 1986.
[26] C.T. Retnner, H.E. Pfnur, D.J. Auerbach, Phys. Rev. Lett. 54 (1985) 2716.
[27] M.B. Lee, Q.Y. Yang, S.T. Ceyer, J. Chem. Phys. 87 (1987) 2724.
[28] A.C. Luntz, D.S. Bethune, J. Chem. Phys. 90 (1989) 1274.
[29] M. Valden, J. Pere, N. Xiang, M. Pessa, Chem. Phys. Lett. 257 (1996) 289.
[30] D.C. Seets, M.C. Wheeler, C.B. Mullins, Chem. Phys. Lett. 266 (1997) 431.
[31] J.H. Larsen, P.M. Holmblad, I. Chorkendorff, J. Chem. Phys. 110 (1999) 2637.
[32] D.W. Goodman, J. Phys. Chem. 100 (1996) 13090.
[33] D.R. Kahn, E.E. Peterson, G.A. Samorjai, J. Catal. 34 (1974) 294.
[34] D.W. Goodman, R.D. Kelley, T.E. Madey, J.T. Yates, J. Catal. 63 (1980) 226.
[35] C.T. Campbell, Adv. Catal. 36 (1989) 1.
[36] F.C. Schouten, E.W. Kalereld, G.A. Bootsma, Surf. Sci. 63 (1977) 460.
[37] F.C. Schouten, O.L.J. Gijzeman, G.A. Bootsma, Bull. Soc. Chim. Belg. 88 (1979) 541.
[38] F.C. Schouten, O.L.J. Gijzeman, G.A. Bootsma, Surf. Sci. 87 (1979) 1.
[39] T.P. Beebe Jr., D.W. Goodman, B.D. Kay, J.T. Yates Jr., J. Chem. Phys. 87 (1987) 2305.
[40] A.V. Hamza, R.J. Madix, 179 (1987) 25.
[41] J.D. Beckerle, A.D. Johnson, Q.Y. Yang, S.T. Ceyer, J. Chem. Phys. 91 (1989) 5756.
[42] Q.Y. Yang, A.D. Johnson, K.J. Maynard, S.T. Ceyer, J. Am. Chem. Soc. 111 (1989) 8748.
[43] S.T. Ceyer, Langmuir 6 (1990) 82.
[44] L. Hanley, Z. Xu, J.T. Yates Jr., Surf. Sci. 248 (1991) L265.

[45] R.P.H. Gasser, An Introduction to Chemisorption and Catalysis by Metals, Clarendon, Oxford, 1985.
[46] X. Jiang, D.W. Goodman, Catal. Lett. 4 (1990) 173.
[47] D.W. Goodman, M. Kiskinova, Surf. Sci 105 (1981) L265.
[48] D.W. Goodman, Acct. Chem. Res. 17 (1984) 194.
[49] M. Kiskinova, D.W. Goodman, Surf. Sci. 108 (1981) 64.
[50] A. Frennet, G. Lienard, A. Crucq, L. Degols, Surf. Sci. 80 (1979) 412.
[51] R.A. Campbell, J. Szanyi, P. Lenz, D.W. Goodman, Catal. Lett. 17 (1993) 39.
[52] P.M. Holmblad, J. Wambach, I. Chorkendorff, J. Chem. Phys. 102 (1995) 8255.
[53] B.O. Nielsen, A.C. Luntz, P.M. Holmblad, I. Chorkendorff, Catal. Lett. 32 (1995) 15.
[54] R.B. Hall, J.G. Chen, J.H. Hardenbergh, C.A. Mims, Langmuir 7 (1991) 2548.
[55] M. Baumer, D. Cappus, H. Kuhlenbeck, H. J-Freund, G. Wilhelmi, A. Brodde, H. Neddermeyer, Surf. Sci. 253 (1991) 116.
[56] L.B.F. Juurlink, P.R. McCabe, R.R. Smith, C.L. Dicologero, A.L. Utz, Phys. Rev. Lett. 83 (1999) 868.
[57] M. Belqued, H. Amariglio, P. Pareja, A. Amariglio, J. Saint-Just, Catal. Today 13 (1992) 437.
[58] M.-C. Wu, D.W. Goodman, J. Am. Chem. Soc. 116 (1994) 1364.
[59] P. L-Solomun, M.-C. Wu, D.W. Goodman, Catal. Lett. 25 (1994) 75.
[60] M.-C. Wu, P. L-Solomun, D.W. Goodman, J. Vac. Sci. Technol. 12 (1994) 2205.
[61] M.M. Koranne, G.W. Zajac, D.W. Goodman, Catal. Lett. 30 (1995) 219.
[62] M.-C. Wu, Q. Xu, D.W. Goodman, J. Phys. Chem. 98 (1994) 5104.
[63] D.W. Goodman, J.M. White, Surf. Sci. 90 (1979) 201.
[64] F.J. Himpsel, K. Christmann, P. Heimann, O.E. Eastman, P.J. Feibelman, Surf. Sci. 115 (1982) L159.
[65] M.-C. Wu, D.W. Goodman, Surf. Sci. 306 (1994) L529.
[66] T. Koerts, M.J. Deelen, R.A. van Santen, J. Catal. 138 (1992) 101.